Sweriduk, G. D., Cheng, V. H. L., Andre, A. D., and Foyle, D. C. (2007). Proceedings of the 26th Digital Avionics Systems Conference, Dallas, TX, Oct. 21, 2007

AUTOMATION TOOLS FOR HIGH-PRECISION TAXIING

G. D. Sweriduk, V. H. L. Cheng, Optimal Synthesis Inc., Palo Alto, CA

A. D. Andre, Interface Analysis Associates, Gilroy, CA

D. C. Foyle, NASA Ames Research Center, Moffett Field, CA

Abstract

Airport congestion is a growing problem, as most air travelers can attest. Efforts are now under way to reduce congestion by increasing the traffic flow rate at airports through the use of automation tools. Which runway and taxiways an aircraft occupies, and when, must be precisely scheduled and executed. Presented herein are results on developing a system which can generate a 4-D trajectory and follow the trajectory accurately.

Introduction

The rapid increase in air travel over the last decade is leading to problems with airport congestion which will only get worse in the future, if predictions are accurate. As a result, airports are being expanded to handle more flights, and new technologies are being developed to reduce the separation between flights. These changes will mean more surface traffic that needs to be managed, and managed more carefully. With more runways there will be more runway crossings required of taxiing aircraft, and with reduced separation, the time window for crossing a runway will be reduced. The greater complexity and requirement for greater precision could overwhelm a system that relies solely on human inputs. In order to enable efficient and safe operations in this more dynamic and complex environment, new tools are needed for both the airport control tower and the cockpit. This paper will present ongoing research into the surface traffic control problem and the development of state-of-the-art technologies to enable aircraft to execute high-precision taxi operations.

Parallel research efforts are aimed at path planning for the movement of arrivals and departures to minimize transit times to and from the gate. The goal of that work is to produce taxi clearances with route and timing information that the control tower will issue to aircraft on the ground or on final approach. The focus of this research is on a system for generating and following 4-D trajectories to achieve the throughput gains made possible by the path planning. This system, called FARGO (Flight-deck Automation for Reliable Ground Operation), uses information about the airport geometry, the aircraft's characteristics, and passenger comfort, as well as the taxi clearance, to generate position and velocity time histories. The flight crew then has the option of following the trajectory in manual mode via specially designed cockpit displays, or in fully automatic mode. The automatic mode uses a nonlinear controller employing the feedback linearization method to track the desired trajectory. Another aspect of this research is to develop contingencies to ensure safe operations in the event that an aircraft deviates from its intended trajectory. Simulations with a high-fidelity model of a Boeing 737 are used to demonstrate the system.

Trajectory Control

The taxi clearance issued by the control tower to an aircraft contains a trajectory as a list of taxiways. These clearances are issued verbally under the present system, although in the system being developed, clearances will be issued digitally. In this way the flight crew does not have to enter the clearance into the trajectory-following system manually. It is also expected to be faster, and easier for flight crews to understand if they can see a string of text. Currently clearances are issued without any timing information, but it is anticipated that in the future, through the use of other computer-aided traffic management tools, the clearance will have timing information. In this work it is assumed that the timing information is included. Given the geometry of the airport, positions and speeds as a function of time can be extracted from the clearance. (Note: the terminology that has been adopted refers to the trajectory as 4-dimensional (4-D), although the altitude coordinate is superfluous since the aircraft is only taxiing.)

Trajectory Generation

Given a clearance string, such as: "TAXI VIA 17C-35C/M5/EM CR 113," and a database of the airport's runways and taxiways, one can generate an array of nodes; i.e.: [180 181 182 183 232 174 162 146 128 113], each of which corresponds to an intersection along the way. To generate an x-y trajectory, it is necessary to know details about how taxiways are designed in order to get the correct turn radii; high-speed exits from runways are laid out using an Euler's spiral [1]. Figure 1 shows the corresponding route for the given clearance for the simulated airport, which is a reasonably accurate representation of the Dallas-Fort Worth airport. Velocities are determined from standard taxiing speeds, acceleration limits, and any time restrictions that might be placed on the route.

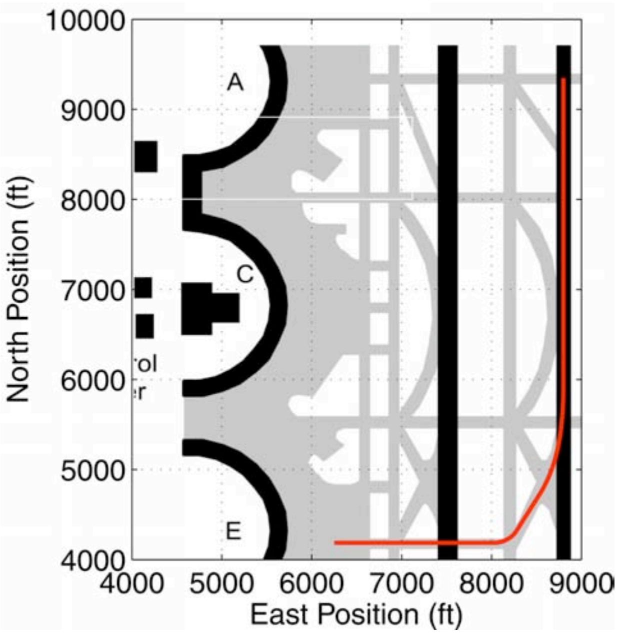

Figure 1. Clearance Route

System Dynamics

The control problem, then, is to get the aircraft to track the 4-D trajectory. The tracking problem was converted to a regulation problem by defining the error dynamics, and designing a controller to regulate the error states to the origin.

The dynamics of the taxiing aircraft are nonlinear and of the general form:

$$\dot{x} = f(x,u) \tag{1}$$

where the state variables are north position (y_I), east position (x_I), north velocity ($\dot{y}_I$), east velocity ($\dot{x}_I$), and the control inputs are throttle, brakes, and tiller (nose wheel angle). In reality the left and right brakes can be used differentially for steering, but in this work they are assumed to act symmetrically. Furthermore, to make the control problem more tractable, the throttle and brakes were ganged together to form a pseudo-control for longitudinal acceleration that can take on positive and negative values. Control effort was allocated to brakes or throttle depending on the sign of the pseudo-control (see Figure 2).

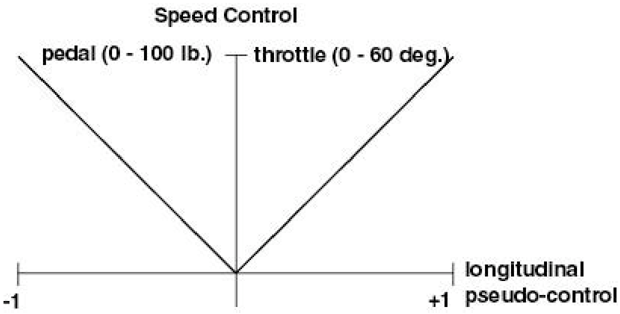

Figure 2. Pseudo-control Allocation

The clearance trajectory gives the desired values of the state variables. However, the state variables are in an inertial frame, and from a control point of view, it makes more sense to deal with quantities in the aircraft's frame of reference. Also, it is more practical to control the trajectory of the aircraft's nose wheel rather than its center of mass, which is what the equations of motion being integrated in the simulation produce.

The desired trajectory is used to define a moving reference frame. This reference frame can be thought of as a body-fixed frame of a phantom aircraft, whose origin is at its center of mass. The nose wheel is located at a known distance along the longitudinal axis of this frame. The error between the actual nose wheel states and the reference nose wheel states can then be expressed as longitudinal and lateral errors in the actual aircraft's body-fixed frame.

The frames of interest are shown in Figure 3. The inertial frame, or runway frame, is shown in the lower left corner of the figure. The dashed line shows the desired trajectory that is traced by the point n_R, which is the reference nose wheel. The body frame (x_B, y_B) is the standard frame used in flight mechanics where the origin is at the center of gravity, the x axis is aligned with the centerline of the fuselage, and the y axis is positive on the right side of the aircraft. The point *n* is the nose wheel position in the body frame. The objective is to regulate the error vector between the points *n* and n_R and its derivative.

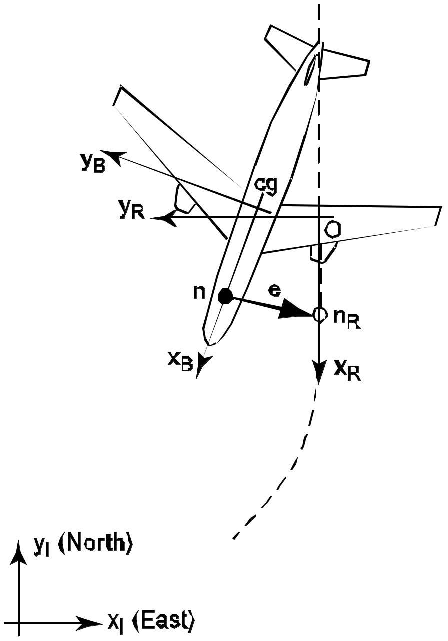

Figure 3. Error Between Aircraft and Reference Trajectory

The error vector is:

$$e = r^{n_R} - r^n \tag{2}$$

where r^{n_R} is the position of n_R in the body frame and r^n is the position of *n* in the body frame. Taking the derivative in the body frame (indicated by the superscript *B*) produces:

$$^{B}\frac{d}{dt}e = {}^{B}\frac{d}{dt}r^{n_R} - {}^{B}\frac{d}{dt}r^{n} = {}^{B}v^{n_R} - 0 \tag{3}$$

The velocity of the nose wheel reference point n_R relative to the body frame can be obtained from the expression for the velocity of the nose wheel reference point relative to the inertial frame:

$$^{I}v^{n_R} = {}^{I}v^{\bar{n}_R} + {}^{B}v^{n_R} \tag{4}$$

or

$$^{B}v^{n_R} = {}^{I}v^{n_R} - {}^{I}v^{\bar{n}_R} \tag{5}$$

where ${}^{I}v^{\bar{n}_R}$ is the inertial velocity of a point $\bar{n}_R$ fixed in the body frame which is coincident with the point n_R in the reference frame at a given instant in time. The inertial velocity of n_R is:

$$^{I}v^{n_R} = {}^{I}v^{O} + {}^{I}\omega^{R} \times r^{On_R} \tag{6}$$

where ${}^{I}v^{O}$ is the inertial velocity of the origin of the reference frame, ${}^{I}\omega^{R}$ is the angular velocity of the reference frame relative to the inertial frame, which can be determined from the reference trajectory, and r^{On_R} is the position vector of the nose wheel reference point in the reference frame, which is known from the aircraft geometry. It should be noted that the first term on the right hand side is given in inertial coordinates while the second term is computed in reference frame coordinates, so a transformation is necessary to perform the addition correctly. The inertial velocity of the point $\bar{n}_R$ is:

$$^{I}v^{\bar{n}_R} = {}^{I}v^{cg} + {}^{I}\omega^{B} \times r^{cg\bar{n}_R} \tag{7}$$

where ${}^{I}v^{cg}$ is the inertial velocity of the c.g. (center of gravity) of the aircraft, ${}^{I}\omega^{B}$ is the angular velocity of the aircraft relative to the inertial frame, and $r^{cg\bar{n}_R}$ is the position vector of $\bar{n}_R$ relative to the aircraft's c.g. Again, the first term on the right hand side is given in inertial coordinates while the second term is computed in body frame coordinates, so a transformation is necessary to perform the addition correctly. The position vector $r^{cg\bar{n}_R}$ can be expressed in the body frame as:

$$r^{cg\bar{n}_R} = r^{cgO} + r^{O\bar{n}_R} = C_{BI}\left(r^{O} - r^{cg}\right) + C_{BR}r^{On_R} \tag{8}$$

where C_{BI} and C_{BR} are transformation matrices to the body frame from the inertial and trajectory reference frames, respectively, r^O is the position of the origin of the reference frame in the inertial frame, and r^{cg} is the position of the c.g. in the inertial frame.

Differentiating the expression for velocity, the acceleration is:

$$ {}^B a^{n_R} = {}^I a^{n_R} - {}^I a^{\bar{n}_R} - 2\,{}^I\omega^B \times {}^B v^{n_R} \tag{9} $$

where

$$ {}^I a^{n_R} = {}^I a^O + {}^I\omega^R \times \left({}^I\omega^R \times r^{On_R}\right) + {}^I\alpha^R \times r^{On_R} \tag{10} $$

$$ {}^I a^{\bar{n}_R} = {}^I a^{cg} + {}^I\omega^B \times \left({}^I\omega^B \times r^{cg\bar{n}_R}\right) + {}^I\alpha^B \times r^{cg\bar{n}_R} \tag{11} $$

${}^I a^O$ and ${}^I a^{cg}$ are the inertial accelerations of the origins of the reference and body frames, respectively, and ${}^I\alpha^R$ and ${}^I\alpha^B$ are the angular accelerations of the reference and body frames, respectively, relative to the inertial frame. In the reference trajectory, turns are made at constant speed, so the angular acceleration ${}^I\alpha^R$ is zero except instantaneously at the beginning and end of a turn.

It is assumed that the trajectory generator generates the inertial position, velocity, and acceleration of the nose wheel, so it is not necessary to compute them using the equations above.

For reasons explained in the following, first-order linear dynamics were added at the inputs, so that the augmented system is linear with respect to the inputs. The additional dynamics could be considered as filters or actuator dynamics.

$$ u(s) = \frac{a}{s+a} u_c(s) \tag{12} $$

where u_c is the output of the controller, and the pole is at $-a$, and a is chosen to be sufficiently large that the dynamics of the filters do not interact with the dynamics of the aircraft. In this case $a = 20$.

Numerical Nonlinear Control

A controller was developed using the feedback linearization methodology [2,3]. The feedback linearization of the dynamics is achieved by redefining the system dynamics in terms of derivatives of the error states. It may be observed from the preceding formulation that the control variables will appear in the third derivative of the position errors. Hence, feedback linearization can be achieved by redefining the dynamics in terms of the position errors and three of its successive time derivatives as the state variables.

Starting from Equation (2), it can be seen that the error states are functions of position, say

$$ e = f_1\left(r^n\right) \tag{13} $$

Differentiating this expression three times will produce a complex expression of the form:

$$ \dddot{e} = \phi(\cdot) + \psi(\cdot) u_c \tag{14} $$

where $\phi(\cdot)$ and $\psi(\cdot)$ are complex nonlinear functions that depend on the state variables. Defining new state variables as $z = \begin{bmatrix} e & \dot{e} & \ddot{e} \end{bmatrix}^T$, the dynamics can be recast in the form:

$$ \dot{z} = Az + Bv \tag{15} $$

where

$$ A = \begin{bmatrix} 0 & 1 & 0 \\ 0 & 0 & 1 \\ 0 & 0 & 0 \end{bmatrix}, \; B = \begin{bmatrix} 0 \\ 0 \\ 1 \end{bmatrix} \tag{16} $$

and the transformed control variable v is given by:

$$ v = \phi(\cdot) + \psi(\cdot) u_c \tag{17} $$

In this work, Nonlinear Synthesis Tools, software for numerically computing the feedback control signals, was used [4]. The nonlinear control system design software automatically constructs the nonlinear functions $\phi(\cdot)$ and $\psi(\cdot)$ from an embedded model of the aircraft. An assumption of the numerical method used is that the control appears linearly in the dynamics in order to obtain the form of Equation 17. To address this problem, the dynamics shown in Equation 12 were added.

Since the transformed system is in a linear, time-invariant form with respect to the transformed control variable, linear control techniques can be used to design a stable feedback control law; i.e.:

$$ v = [k_1 \;\; k_2 \;\; k_3]\, z \tag{18} $$

In this study, pole placement was used to compute the gains using standard techniques. The actual control variables can be recovered from the transformed control variables using the inverse relationship from (17):

$$u_c = \psi^{-1}(\cdot)[v - \phi(\cdot)] \qquad (19)$$

If the system nonlinearities $\phi(\cdot)$ and $\psi(\cdot)$ are known reasonably well, the resulting closed-loop system will have dynamic properties close to the transformed system.

Due to the assumptions of the numerical method, the embedded model needed to be modified. Both the throttle and brake responses are nearly constant for inputs between 0 and about 10%. This is practically the same situation as a saturated actuator, and leaves the system effectively uncontrollable. To avoid this problem, curves were fitted to the throttle and brake response, but were given more slope near zero (see Figure 4 and Figure 5). These curves were then substituted in the embedded model for the actual dynamics.

In the design model, the angular acceleration is always assumed to be zero.

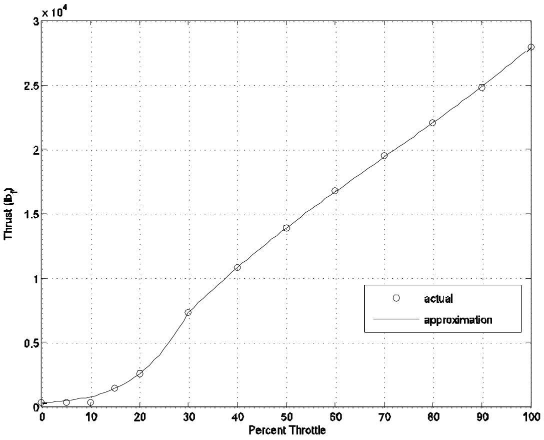

Figure 4. Throttle Function Approximation

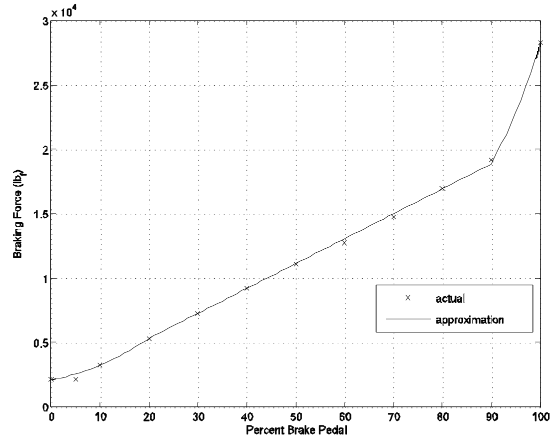

Figure 5. Brake Function Approximation

The poles selected for the lateral channel were [-2, -3, -20]. The poles selected for the longitudinal channel were [-1, -2, -20] when the aircraft was taxiing, and during rollout the poles were a function of total velocity: [σ, 2σ, -20] where:

$$\sigma = -\left(1 - exp\left(-\frac{v_{TD} - v}{20}\right)\right) \qquad (20)$$

and v_{TD} = 205.0 is the touchdown velocity.

Figure 6 shows the desired and actual trajectories in the horizontal plane. The total velocity is shown in Figure 7. It can be seen that the aircraft comes to a stop midway because it crosses another runway. Figure 8 shows the x and y axis errors in nose wheel position, in the body frame. It can be seen that the error never exceeds about 2.5 feet for the given choice of poles. From Figure 9 it can be seen that the velocity errors never exceed about 2 feet/second. The largest errors occur around the time that the aircraft starts moving from rest. The body-frame accelerations are shown in Figure 10 and show that the peak longitudinal acceleration is approximately 0.2 g, and the peak lateral acceleration is approximately 0.1 g. The time histories of the control inputs are shown in Figure 11. The control allocation scheme created some undesirable switching behavior. In the future a better blending scheme will be required.

Conclusions

Initial development of automated taxiing tools was presented. Taxi clearances from the tower were converted into time-dependent ground trajectories. A nonlinear controller was developed for a taxiing aircraft that can accurately follow a trajectory as a function of time.

References

[1] Federal Aviation Administration, 1989, Airport Design, Advisory Circular 150/5300-13, Washington, D. C., U.S. Dept. of Transportation.

[2] Isidori, A., 1989, Nonlinear Control Systems - An Introduction, New York, NY, Springer-Verlag, pp. 145-172.

[3] Marino, R., and P. Tomei, 1995, Nonlinear Control Design, New York, NY, Prentice Hall, pp. 41-60.

[4] Menon, P. K., et al., 2000, Nonlinear Synthesis Tools™ for Use with MATLAB®, Palo Alto, CA, Optimal Synthesis Inc.

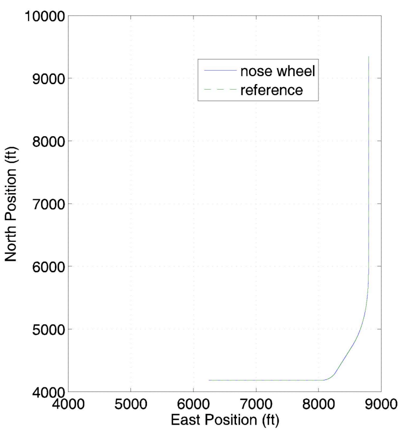

Figure 6. North Position vs. East Position

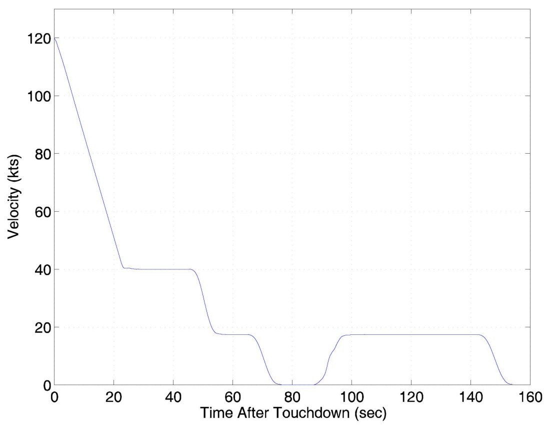

Figure 7. Total Velocity vs. Time

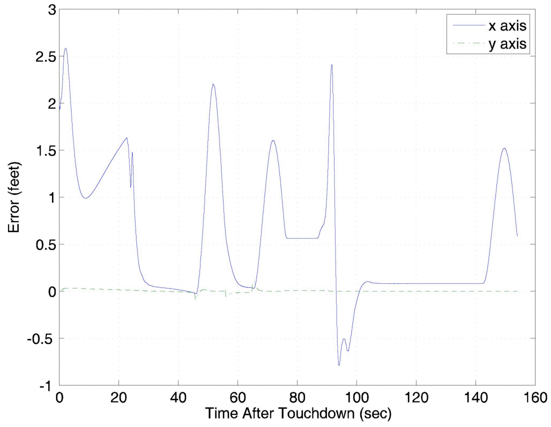

Figure 8. Longitudinal and Lateral Position Error vs. Time

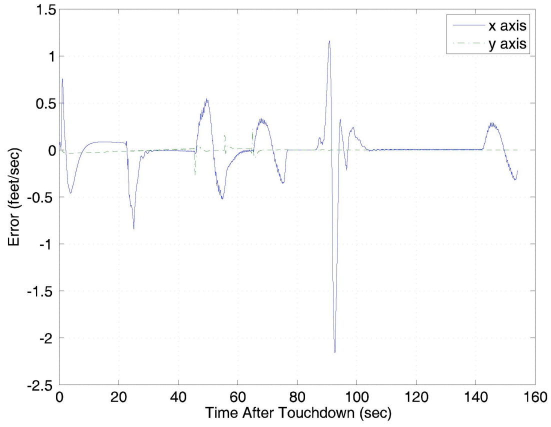

Figure 9. Longitudinal and Lateral Velocity Error vs. Time

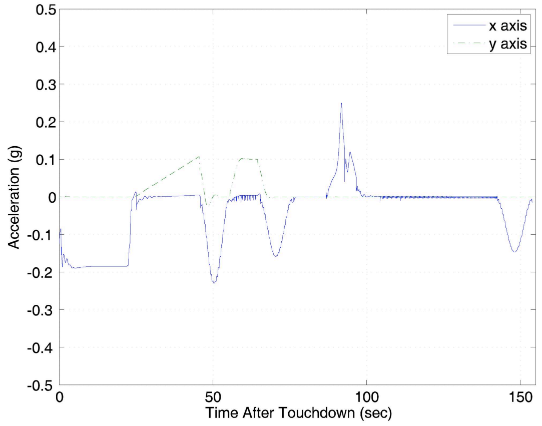

Figure 10. Longitudinal and Lateral Acceleration vs. Time

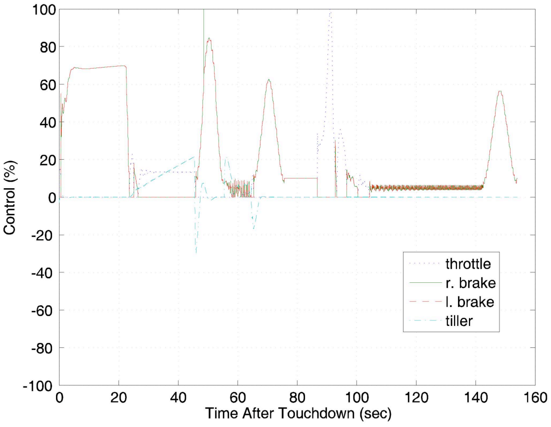

Figure 11. Control Inputs vs. Time

Acknowledgements

This work was supported by NASA under the Small Business Innovations Research program, contract no. NNA06AA06C